

# Direct Solid-State NMR Spectroscopic Evidence for the $\text{NH}_4\text{AlF}_4$ Crystalline Phase Derived from Zeolite HY Dealuminated with Ammonium Hexafluorosilicate

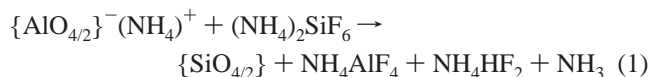
Hsien-Ming Kao\* and Pai-Ching Chang

Department of Chemistry, National Central University, Chung-Li, Taiwan 32054, R.O.C.

Received: August 1, 2006; In Final Form: August 28, 2006

Multinuclear  $^1\text{H}$ ,  $^{19}\text{F}$ , and  $^{27}\text{Al}$  MAS (magic angle spinning) and corresponding 2D HETCOR (heteronuclear correlation) NMR spectroscopy, in combination with powder XRD measurements, provide the direct evidence for the  $\text{NH}_4\text{AlF}_4$  crystalline phase, which was formed from zeolite HY dealuminated with an aqueous  $(\text{NH}_4)_2\text{SiF}_6$  solution at 80 °C. The  $\text{NH}_4\text{AlF}_4$  crystalline phase exhibits a characteristic second-order quadrupolar-induced  $^{27}\text{Al}$  NMR line shape spreading from 0 to  $-90$  ppm (in a magnetic field of 11.7 T) and two  $^{19}\text{F}$  resonances at  $-151$  and  $-166$  ppm in the  $^{19}\text{F}$  NMR spectrum. An  $^{27}\text{Al}$  quadrupolar coupling constant ( $C_Q$ ) of 9.5 MHz and an asymmetry parameter ( $\eta$ ) of 0.1 were identified, for the first time, for the  $\text{NH}_4\text{AlF}_4$  crystalline phase observed. On the basis of the  $^{19}\text{F}\{^{27}\text{Al}\}$  TRAPDOR (transfer population in double resonance) NMR results, the  $^{19}\text{F}$  resonances at  $-151$  and  $-166$  ppm are therefore assigned to  $^{19}\text{F}$  spins associated with the fluorines in the terminal  $\text{Al}-\text{F}$  and the bridging  $\text{Al}-\text{F}-\text{Al}$  groups, respectively.

Dealumination is an important process that allows adjustments in the Si/Al ratio of zeolites, hence their acidity and catalytic properties. For example, the dealumination of zeolite Y not only improves its hydrothermal stability but also influences its catalytic cracking properties. Therefore, the dealumination process has been a matter of considerable interest for applications of zeolitic materials. Depending on the methods of dealumination, for example, hydrothermal/thermal treatment,<sup>1</sup> acid leaching,<sup>2</sup> and chemical treatments,<sup>3</sup> extraframework aluminum (EFAl) species are often formed inside the zeolite structure. These EFAl species may change the acidic properties of zeolites dramatically. Several forms of the EFAl species have been proposed in the literature:<sup>4</sup> cationic species such as  $\text{Al}^{3+}$ ,  $\text{AlO}^+$ ,  $\text{Al}(\text{OH})^{2+}$ , and  $\text{Al}(\text{OH})_2^+$  and neutral or polymeric species such as  $\text{AlO}(\text{OH})$ ,  $\text{Al}(\text{OH})_3$ , and  $\text{Al}_2\text{O}_3$ . However, the exact nature of the EFAl species formed during the dealumination process of zeolites still remains unclear partially due to lack of direct spectroscopic evidence. In 1983, Skeels and Breck<sup>5</sup> reported the fluorosilicate method for the dealumination of medium- and large-pore zeolites with aqueous solutions of ammonium hexafluorosilicate  $(\text{NH}_4)_2\text{SiF}_6$ , denoted as AHFS in the presence of ammonium acetate ( $\text{NH}_4\text{OAc}$ ) for controlling the pH of the solution. The advantages, limitations and fields of applicability of this dealumination technique have been recently reviewed.<sup>6</sup> Clear evidence for the removal of aluminum and the isomorphous incorporation of silicon into the zeolite framework has been established. However, the critical choices of the operating conditions and reaction parameters have been emphasized.<sup>5</sup> Recently, a modified technique based on the thermal treatment of ground mixtures of zeolite  $\text{NH}_4\text{Y}$  and crystalline AHFS in the solid state has been reported.<sup>7</sup> The reaction has been proposed to proceed according to



where  $\{\text{AlO}_{4/2}\}^-$  and  $\{\text{SiO}_{4/2}\}$  refer to primary tetrahedral T sites of zeolite structures. In a previous study of fluorination of alumina with high levels of  $\text{NH}_4\text{F}$ , DeCanio et al.<sup>8</sup> also proposed the formation of  $\text{NH}_4\text{AlF}_4$  salts on the surface of fluorinated alumina. However, both studies did not provide direct spectral evidence for the formation of  $\text{NH}_4\text{AlF}_4$ . This is partially due to the lack of a precise identification method for aluminum fluoride species, which may be present at low concentrations and in an amorphous state. Moreover, structural identification is often complicated by the rich structural chemistry of the aluminum oxy/hydroxyfluorides. Some of fluorinated phases are structurally closely related, making their identification difficult. As the acidic properties and catalytic activity of zeolites are often affected by the presence of the EFAl species, identification of these fluorine-containing EFAl species is critical to the understanding of the structural properties induced by the AHFS treatment. A full characterization of the state and nature of fluorinated EFAl species formed during the AHFS dealumination process still remains to be determined. Solid-state NMR spectroscopy has been recognized as a powerful tool for probing the local environment of a particular nucleus and is ideally suited to study these fluorinated EFAl species. This prompted us to conduct a study of zeolite HY dealuminated with AHFS by multinuclear solid-state  $^1\text{H}$ ,  $^{19}\text{F}$  and  $^{27}\text{Al}$  MAS (magic angle spinning) and their corresponding 2D HETCOR (heteronuclear correlation) NMR, in combination with powder XRD (X-ray diffraction) measurements.

The parent zeolite HY was obtained from Zeolyst (CBV600, Si/Al = 2.6). The standard AHFS dealumination method of Skeels and Breck<sup>5</sup> was slightly modified to dealuminate HY in the present study. Typically, 1 g of HY was preheated at 80 °C

\* Corresponding author. E-mail: hmkao@cc.ncu.edu.tw; Fax: +886-3-4227664; Phone: +886-3-4275054.

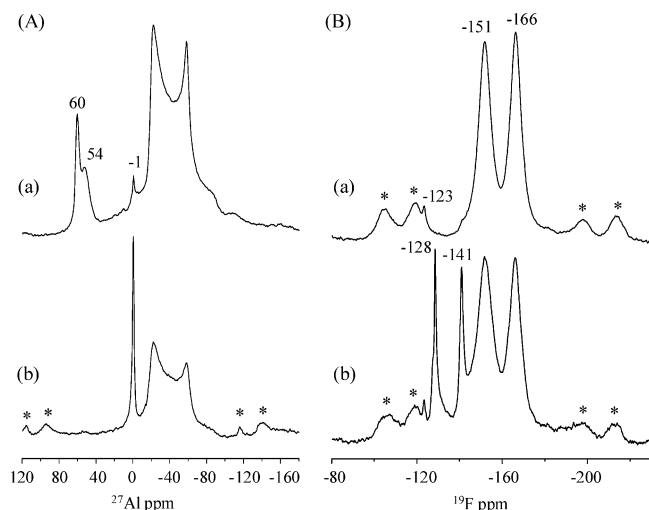


**Figure 1.** (A)  $^{27}\text{Al}$  and (B)  $^{19}\text{F}$  MAS NMR spectra of (a) HY/AHFS-0.5 and (b) HY/AHFS-1.6.  $^{27}\text{Al}$  MAS NMR spectra were obtained with a small flip angle of approximately  $15^\circ$  ( $0.6\ \mu\text{s}$ ) and with a repetition time of 2 s.  $^{19}\text{F}$  MAS NMR spectra were acquired with a rotor synchronized spin-echo sequence with an echo time of  $45.4\ \mu\text{s}$  ( $\nu_r = 22\ \text{kHz}$ ) and a repetition time of 15 s. Asterisks denote spinning sidebands. The  $^{27}\text{Al}$  and  $^{19}\text{F}$  chemical shifts are referenced to 1.0 M aqueous aluminum sulfate and hexafluorobenzene as external standards at 0.0 and  $-163\ \text{ppm}$ , respectively.

in 50 mL distilled water, in the absence of  $\text{NH}_4\text{OAc}$ , followed by the dropwise addition of 10 mL aqueous AHFS solution with various concentrations over a period of 1 h. The solution was then maintained at  $80\ ^\circ\text{C}$  with constant stirring for another 3 h. The resulting solution was cooled to room temperature, filtered, and then dried at  $60\ ^\circ\text{C}$  overnight. In contrast to the standard procedure of AHFS treatment, the dealuminated samples obtained were not washed by hot water in order to reserve all the EFAl species for characterization. These dealuminated samples were designated as HY/AHFS- $x$ , where  $x$  denotes the molar ratio of AHFS to the total Al content of the parent zeolite.

Figure 1 shows the  $^{27}\text{Al}$  and  $^{19}\text{F}$  MAS NMR spectra, acquired on a Varian Infinityplus-500 spectrometer equipped with a Chemagnetics HFX 3.2 mm quadrupole-resonance probe, of HY treated with various AHFS contents. At low AHFS loading ( $x = 0.5$ ), the signal at 60 ppm of the parent HY, attributed to four-coordinated aluminum, was split into two peaks at 60 and 54 ppm after AHFS dealumination. A broad pattern spreading from 0 to  $-90\ \text{ppm}$  (denoted as site I), characteristic of second-order quadrupolar interaction effects on the central transition of aluminum, and a small peak at  $-1\ \text{ppm}$  were also observed. The corresponding  $^{19}\text{F}$  NMR spectrum (part a of Figure 1B, collected using a Hahn echo sequence) shows two major peaks at  $-151$  and  $-166\ \text{ppm}$  with a shoulder at  $-141\ \text{ppm}$  and a small peak at  $-123\ \text{ppm}$ . With a higher level of AHFS ( $x = 1.6$ ), the peaks due to the framework tetrahedral aluminum were no longer observed, indicating a complete destruction of HY structure, as confirmed by XRD (X-ray diffraction) measurements. Two major  $^{27}\text{Al}$  resonances were observed for this sample, one sharp peak at  $-1\ \text{ppm}$  and the other is due to site I. The corresponding  $^{19}\text{F}$  NMR spectrum shows similar features with HY/AHFS-0.5, except for a new peak at  $-128\ \text{ppm}$  due to the residual AHFS.

The peaks at  $-1\ \text{ppm}$  in the  $^{27}\text{Al}$  NMR spectra and at  $-141\ \text{ppm}$  in the  $^{19}\text{F}$  NMR spectra match well with the positions of  $^{27}\text{Al}$  and  $^{19}\text{F}$  resonances in  $(\text{NH}_4)_3\text{AlF}_6$ .<sup>9</sup> The presence of  $(\text{NH}_4)_3\text{AlF}_6$  is also confirmed by X-ray diffraction studies, which show small additional peaks at  $2\theta = 17^\circ$  and  $20^\circ$  that

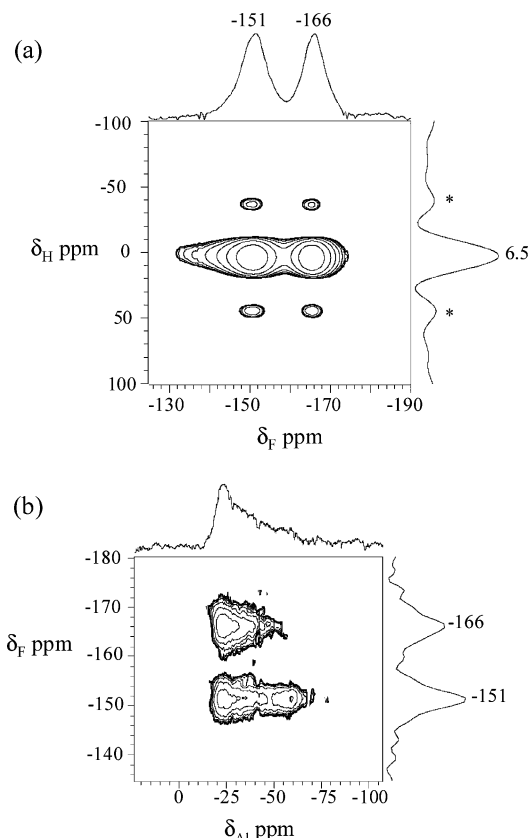


**Figure 2.** (a)  $^{19}\text{F}\{^1\text{H}\}$  and (b)  $^{27}\text{Al}\{^{19}\text{F}\}$  HETCOR NMR spectra, where the nuclei in the brackets are detected in the  $t_1$  dimension, of the washed HY/AHFS-1.6 sample. Asterisks denote spinning sidebands. The Hartmann–Hahn conditions were determined with  $\text{NH}_4\text{F}_{(s)}$  and anhydrous aluminum fluoride for the  $^{19}\text{F}\{^1\text{H}\}$  and  $^{27}\text{Al}\{^{19}\text{F}\}$  2D HETCOR NMR experiments, respectively. The typical contact time for  $^1\text{H}$  to  $^{19}\text{F}$  and  $^{19}\text{F}$  to  $^{27}\text{Al}$  CP (cross-polarization) was 1.0 and 0.1 ms, respectively, and a repetition time of 1 s was used.

are identical with the typical pattern of  $(\text{NH}_4)_3\text{AlF}_6$ . The peak at  $-123\ \text{ppm}$  is presumably due to the presence of the  $\text{F}^-$  counterion of  $\text{NH}_4^+$  or  $\text{H}^+$  occurring in channels.<sup>9</sup>

The HY/AHFS-1.6 sample can be washed to remove the  $(\text{NH}_4)_3\text{AlF}_6$  phase and to preserve only site I in the  $^{27}\text{Al}$  NMR spectrum and two  $^{19}\text{F}$  resonances at  $-151$  and  $-166\ \text{ppm}$  in the  $^{19}\text{F}$  NMR spectrum, respectively. The  $^{19}\text{F}\{^1\text{H}\}$  and  $^{27}\text{Al}\{^{19}\text{F}\}$  2D HETCOR NMR,<sup>10</sup> where the nuclei in the brackets are detected in the  $t_1$  dimension, were therefore performed on this sample and the spectra are shown in Figure 2. Both HETCOR experiments identify that the  $^{19}\text{F}$  spins are in close proximity to the aluminum spins at site I and the protons in  $\text{NH}_4^+$  groups ( $^1\text{H}\ \delta_{\text{iso}} = 6.5\ \text{ppm}$ ).  $^{27}\text{Al}$  triple-quantum (3Q) MAS NMR<sup>11</sup> results (see Supporting Information, Figure S1) show that there is no distribution of site I, and thus a quadrupole coupling constant ( $C_Q$ ) of  $9.5 \pm 0.5\ \text{MHz}$ ,  $\delta_{\text{iso}} = -5 \pm 0.5\ \text{ppm}$  and the asymmetry parameter ( $\eta$ ) of  $0.1 \pm 0.1$  can be obtained from the simulation by using the STARS software.<sup>12</sup>

Given that the line width and line shape of  $^{27}\text{Al}$  NMR signals is very sensitive to the coordination environment around the aluminum atom. The characteristic second-order quadrupolar induced line shape of site I suggests that the EFAl species may come from a crystalline phase. To test this proposal, powder XRD measurements were performed on the washed HY/AHFS-1.6 sample and the XRD pattern was shown in the part a of Figure 3A. The pattern matched well with that of  $\text{NH}_4\text{AlF}_4$  while comparing to the Joint Committee for Powder Diffraction Sources (JCPDS) files (20-0077). To further confirm the

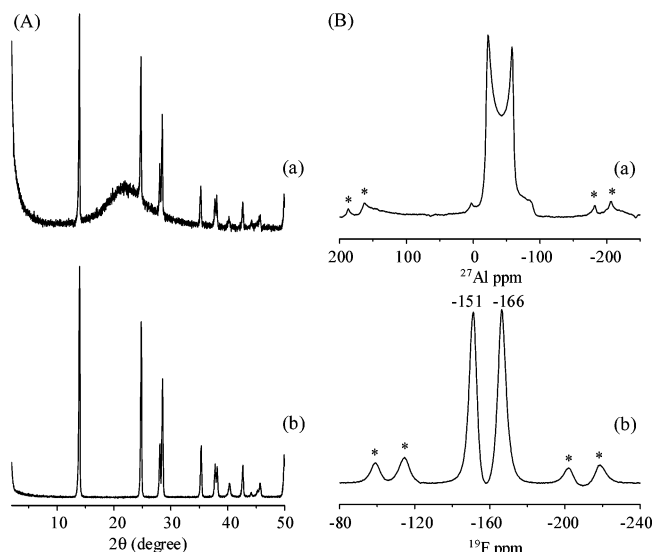


**Figure 3.** (A) Powder XRD patterns of (a) the washed HY/AHFS-1.6 sample and (b)  $\text{NH}_4\text{AlF}_4(\text{s})$  and (B)  $^{27}\text{Al}$  (top) and  $^{19}\text{F}$  (bottom) MAS NMR spectra of  $\text{NH}_4\text{AlF}_4(\text{s})$ . Asterisks denote spinning sidebands.

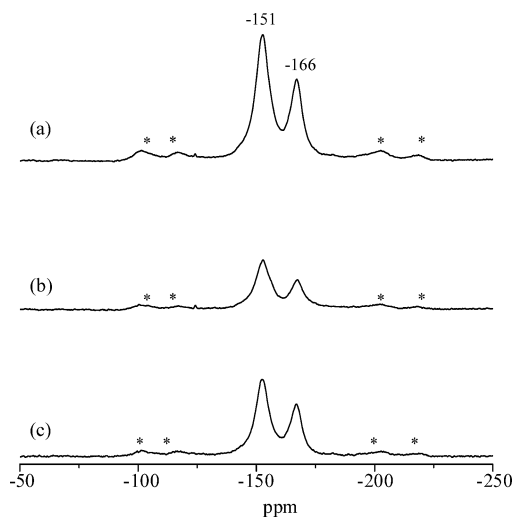


**Figure 4.**  $^{19}\text{F}\{^{27}\text{Al}\}$  TRAPDOR NMR spectra of the washed HY/AHFS-1.6 sample, (a) without and (b) with  $^{27}\text{Al}$  on-resonance irradiation (r.f. field strength = 85 kHz,  $\tau$  = 166  $\mu\text{s}$ , spinning speed = 24 kHz). The difference spectrum is shown in (c). Asterisks denote spinning sidebands.

formation of  $\text{NH}_4\text{AlF}_4(\text{s})$  from zeolite HY dealuminated with AHFS, solid  $\text{NH}_4\text{AlF}_4$  was synthesized by thermal treatment of  $(\text{NH}_4)_3\text{AlF}_6(\text{s})$  at 200  $^\circ\text{C}$  for 12 h.<sup>13</sup> The powder XRD pattern and  $^{27}\text{Al}$  and  $^{19}\text{F}$  MAS NMR spectra of  $\text{NH}_4\text{AlF}_4(\text{s})$ , synthesized from thermal treatment of  $(\text{NH}_4)_3\text{AlF}_6(\text{s})$ , all match with those of site I (part b of Figure 3A and Figure 3B). It is known that the crystal structure of  $\text{NH}_4\text{AlF}_4$  is a layered structure which is formed by layers of  $\text{AlF}_6$  octahedra joined by shared corners, and  $\text{NH}_4^+$  lies between these layers.<sup>13</sup> The  $^{19}\text{F}\{^{27}\text{Al}\}$  TRAPDOR (transfer population in double resonance) NMR<sup>14</sup> results (Figure 4) show that the  $^{19}\text{F}$  resonances at -151 and -166 ppm have TRAPDOR fractions of 58% and 65%, respectively, under conditions of on-resonance  $^{27}\text{Al}$  irradiation (r.f. field strength = 85 kHz,  $\tau$  = 166  $\mu\text{s}$ ) and at a spinning speed of 24 kHz. On basis of the  $^{19}\text{F}\{^{27}\text{Al}\}$  TRAPDOR NMR results, the different TRAPDOR fractions could be a hint that the  $^{19}\text{F}$  resonances at -151 and -166 ppm were due to the fluorines in the terminal Al-F and the bridging Al-F-Al groups of  $\text{NH}_4\text{AlF}_4(\text{s})$ , respectively.

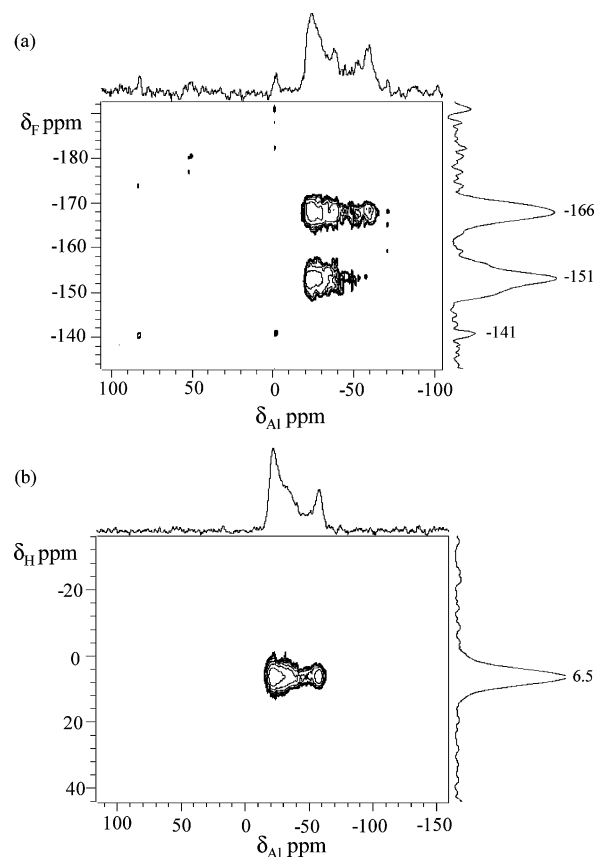


**Figure 5.** (a)  $^{27}\text{Al}\{^{19}\text{F}\}$  and (b)  $^{27}\text{Al}\{^1\text{H}\}$  HETCOR NMR spectra of the HY/AHFS-0.5 sample. The experimental conditions of  $^{27}\text{Al}\{^{19}\text{F}\}$  HETCOR NMR experiments are described in Figure 2b except a longer contact time of 0.2 ms was used. A contact time of 1 ms was used for  $^1\text{H}$  to  $^{27}\text{Al}$  CP process in the  $^{27}\text{Al}\{^1\text{H}\}$  HETCOR NMR experiment. Both spectra were acquired at a spinning speed of 24 kHz.

To probe the proximity between the  $\text{NH}_4\text{AlF}_4$  crystalline phase and the framework of the parent zeolite HY, both  $^{27}\text{Al}\{^{19}\text{F}\}$  and  $^{27}\text{Al}\{^1\text{H}\}$  HETCOR NMR experiments were performed on the HY/AHFS-0.5 sample, and the results are shown in Figure 5. Clearly, both HETCOR NMR experiments show that there is no correlation between the framework tetrahedral Al atoms of the parent zeolite HY and the  $\text{NH}_4\text{AlF}_4$  phase. These observations imply that the  $\text{NH}_4\text{AlF}_4$  phase thus formed is distant from the zeolite framework, and most likely exists as a separate phase. The easy removal of  $(\text{NH}_4)_3\text{AlF}_6(\text{s})$  and good retention of  $\text{NH}_4\text{AlF}_4(\text{s})$  in the dealuminated sample after washing with water could be due to the difference in their solubility in water. Moreover, these HETCOR NMR results also reveal that the possibility for the framework  $^{27}\text{Al}$  atoms that are associated with fluorines can be excluded. On the basis of its larger line width and easier removal from the framework, the  $^{27}\text{Al}$  signal at 54 ppm is assigned to Al in a more distorted tetrahedral environment, which is less tightly bound to the zeolite framework in comparison to that of 60 ppm. The presence of similar Al species has been reported in USY zeolites.<sup>15</sup>

It has been pointed out that the operating conditions are critical for the dealumination of zeolites with AHFS.<sup>5</sup> For comparison purposes, another series of HY/AHFS-*x* were prepared in the presence of  $\text{NH}_4\text{OAc}$ , i.e., by following the method of Skeels and Breck.<sup>5</sup> By measuring the  $^{27}\text{Al}$  and  $^{19}\text{F}$  MAS NMR spectra of these samples, the  $\text{NH}_4\text{AlF}_4$  phase was also detected at a low AHFS loading ( $x$  = 0.3), while  $(\text{NH}_4)_3\text{AlF}_6(\text{s})$  was the dominant species at higher AHFS loadings (see Supporting Information, Figure S2). Although different operation

conditions were employed, some common aluminum fluorides, namely  $\text{NH}_4\text{AlF}_{4(s)}$  and  $(\text{NH}_4)_3\text{AlF}_{6(s)}$ , were formed at various AHFS loadings. This implies that dealumination of zeolite HY with aqueous AHFS solution in the presence and absence of  $\text{NH}_4\text{OAc}$  might consist of a series of common reaction pathways.<sup>7</sup> The relative intensities of these two aluminum fluorides as a function of AHFS loading also suggest a possible transformation process undergoing between  $\text{NH}_4\text{AlF}_{4(s)}$  and  $(\text{NH}_4)_3\text{AlF}_{6(s)}$ . Interestingly, the  $\text{AlO}_{6-x}\text{F}_x$  species often observed in the fluorination of alumina were not observed in the present study.<sup>16</sup> This suggests that the nature and status of the extracted framework Al atoms in HY dealuminated with AHFS should be very different from that of the fluorinated alumina. Further studies are in progress in order to improve the understanding of the nature of the EFAl species and the reaction pathways induced by the AHFS dealumination process.

In conclusion, by a combination of different methods of solid-state NMR spectroscopy and powder XRD measurements, we have identified the formation of  $\text{NH}_4\text{AlF}_4$  crystalline phase, in addition to  $(\text{NH}_4)_3\text{AlF}_{6(s)}$ , which can be derived from zeolite HY dealuminated with an aqueous AHFS solution at 80 °C.

**Acknowledgment.** We thank the National Science Council of Taiwan for financial support.

**Supporting Information Available:** MQMAS NMR spectrum of HY/AHFS-1.6 and  $^{27}\text{Al}$  and  $^{19}\text{F}$  MAS NMR spectra of HY/AHFS- $x$ , prepared in the presence of  $\text{NH}_4\text{OAc}$ . This material is available free of charge via the Internet at <http://pubs.acs.org>.

## References and Notes

- (1) Parikh, P. A.; Subrahmanyam, N.; Bhat, Y. S.; Halgeri, A. B. *J. Mol. Catal.* **1994**, 88, 85.
- (2) Maache, M.; Janin, A.; Lavalley, J. C.; Joly, J. F. *Zeolites* **1993**, 13, 419.
- (3) Weitkamp, J.; Sakuth, M.; Chen, C.; Ernst, S. *Chem. Commun.* **1989**, 1908.
- (4) (a) Shannon, R. D.; Gardner, K. H.; Staley, R. H.; Bergeret, G.; Gallezot, P.; Auroux, A. *J. Phys. Chem.* **1985**, 89, 4778. (b) Kuhl, G. H. In *Molecular Sieves*; Uytterhoeven, J. B., Ed.; Lueven University Press: Leuven, 1973; p 227.
- (5) (a) Skeels, G. W.; Breck, D. W. In *Proceedings of the Sixth International Zeolite Conference*; Olson, D. H., Bisio, A., Eds.; Butterworths: Surrey, 1983; p 87. (b) Breck, D. W.; Blass, H.; Skells, G. W. U.S. Patent 4,503,203, 1985.
- (6) Beyer, H. K. In *Molecular Sieves-Science and Technology*; Karge, H. G., Weitkamp, J., Eds.; Springer: Berlin, 2002; Vol. 3, p 203.
- (7) Pál-Borbély, G.; Beyer, H. K. *Phys. Chem. Chem. Phys.* **2003**, 5, 2145.
- (8) DeCanio, E. C.; Bruno, J. W.; Nero, V. P.; Edwards, J. C. *J. Catal.* **1993**, 140, 84.
- (9) Delmotte, L.; Soulard, M.; Guth, F.; Seive, A.; Lopez, A.; Guth, J. L. *Zeolites* **1990**, 10, 778.
- (10) (a) Caravatti, P.; Braunschweiler, L.; Ernst, R. R. *Chem. Phys. Lett.* **1983**, 100, 305. (b) Vega, A. J. *J. Am. Chem. Soc.* **1998**, 110, 1049.
- (11) (a) Frydman, L.; Harwood, J. S. *J. Am. Chem. Soc.* **1995**, 117, 5367. (b) Amoureux, J. P.; Fernandez, C.; Steuernagel, S. *J. Magn. Reson. Ser. A* **1996**, 123, 116.
- (12) Jakobsen, H. J.; Skibstedt, J.; Bildsoe, H.; Nielsen, N. C. *J. Magn. Reson.* **1989**, 85, 173.
- (13) Shinn, D.; Crockett, D.; Haendler, H. *Inorg. Chem.* **1966**, 5, 1927.
- (14) (a) Grey, C. P.; Vega, A. J. *J. Am. Chem. Soc.* **1995**, 117, 8232. (b) Kao, H.-M.; Grey, C. P. *Chem. Phys. Lett.* **1996**, 259, 459.
- (15) Fyfe, C. A.; Bretherton, J. L.; Lam, L. Y. *J. Am. Chem. Soc.* **2001**, 123, 5285.
- (16) (a) Fischer, L.; Harle, V.; Kasztelan, S.; d'Espinose de la Caillerie, J. B. *Solid State Nucl. Magn. Reson.* **2000**, 16, 85. (b) Chupas, P. J.; Corbin, D. R.; Rao, V. N. M.; Hanson, J. C.; Grey, C. P. *J. Phys. Chem. B* **2003**, 107, 8327.